

Forces between Liquid Interfaces in the Presence of Polymer: Concentration, Solvent, and Mass Effects

A. Espert, P. Omarjee, J. Bibette, F. Leal Calderon, and O. Mondain-Monval*

Centre de Recherche Paul Pascal, CNRS, Av. A. Schweitzer, 33600 Pessac, France

Received March 3, 1998; Revised Manuscript Received June 4, 1998

ABSTRACT: We report surface force measurements between emulsion droplets and flat air–water interfaces (foam films) in the presence of an aqueous statistical copolymer solution (of poly(vinyl alcohol) and poly(vinyl acetate)) in the dilute regime. We observe a repulsive force that is exponentially decaying and that cannot be attributed to electrostatic double-layer repulsion. The qualitative behavior of the repulsive force weakly depends on the polymer concentration, while its range is a function of the polymer average molecular weight that is varied from 10 000 to 155 000. The force is drastically affected when the temperature approaches the Θ point (going from good to Θ conditions). We show that the force range scales as the polymer coil radius of gyration. These results are compared with theoretical predictions.

Introduction

Foams and colloidal dispersions require repulsive surface forces to become metastable. The most important forces that determine their stability are van der Waals forces, electrostatic forces, and also steric forces due to adsorbed polymers. The net force acting between colloidal particles or air bubbles determines their stability. A net attractive force leads to the aggregation of particles. In the case of liquid particles, coalescence may occur when the thin liquid films separating the interfaces break. If the net force is repulsive, the system can remain stable on a given time scale. Force measurement techniques, and especially the so-called surface forces apparatus, have been widely used to understand the interactions between solid surfaces, which give insights into the dispersion stability.¹ Most of the time, electrostatically stabilized dispersions become unstable when the ionic strength of the medium is increased sufficiently, due to the reduction in the spatial extension of electrostatic double layers (screening effect). Hence, one major advantage of using neutral macromolecules as stabilizers is that their repulsive adsorbed layers are less sensitive to electrolyte concentration.² Recently, we have developed a new technique that allows the measurement of forces between colloidal droplets.³ Here, we use this technique and the thin film balance technique⁴ to probe the stability aspects of oil-in-water emulsion and foam liquid films made from polymer solutions.

The essential experimental contribution to the knowledge of the forces behavior between polymer-covered interfaces has been obtained with the surface forces apparatus.⁵ For technical reasons, these studies are restricted to the interactions between solid surfaces with intensities much larger than the thermal excitation. Thus, except for the pioneering experimental work of Lyklema and van Vliet,⁶ few things are known concerning the interactions between fluid interfaces.

In this paper, we present the measurements of repulsive forces that take place between two kinds of fluid interfaces when a statistical neutral copolymer is adsorbed. The measured repulsive force is exponentially decaying. By varying the polymer molecular weight and increasing the solution temperature toward

the Θ temperature (i.e., toward the poor solvent regime in which the gyration radius is significantly reduced), we show that the force range is proportional to the coil radius of gyration. We compare our results to several theories on polymer-induced repulsive forces.

Experimental Section

1. Force Measurement Techniques. First, we present the two different techniques that have allowed the measurements of forces between both oil–water and air–water interfaces.

The force profile between oil droplets is directly measured using the recently developed chaining technique.^{3,7} A magnetic oil (ferrofluid provided by Rhône-Poulenc Co.), octane in which small grains (10 nm in size) of Fe_3O_4 are dispersed, is used to create monodisperse emulsion droplets stabilized with a water soluble surfactant. By imposing a magnetic field, polarized droplet chains align along the field and diffract the light, allowing their spacing to be measured precisely. Since a given field corresponds to an applied known attractive force between droplets, we deduce the opposing repulsive force at various separations. This force profile is measured from the onset of chaining up to the saturation of the ferrofluid magnetization, which corresponds to ratios F/R , where F is the force and R is the droplet radius, that range from 10^{-6} to 10^{-4} N/m. In such a force range, the droplets can be considered as undeformable spheres. That technique allows the direct measurement of the repulsive force–distance profile between individual ferrofluid emulsion droplets having a radius R of around 100 nm. The typical surface separation that can be measured ranges from 1 to about 150 nm with a precision of ± 1 nm. In all experiments, the emulsion volume fraction is low enough (0.1%) to assume that the polymer bulk concentration remains constant (the adsorbed amount is fully negligible).

To measure the disjoining pressure isotherms between air–water interfaces, a modified version of the porous plate technique first developed by Mysels and Jones⁸ has been realized. The modified version includes some improvements made by several authors.⁹

A thick liquid lens is formed in the center of a small hole drilled in a porous glass disk fused to a capillary tube. The disk is enclosed in a 200 cm³ hermetically sealed plexiglass box, with the capillary tube exposed to a constant reference pressure. Under the effect of a constant applied pressure difference ΔP between the box and the reference, the liquid drains and a flat horizontal liquid film is formed. The film can be stabilized at a thickness h if the surface force per unit area balances the pressure difference (ΔP) applied. To prevent

Table 1. Characteristics of Poly(vinyl alcohol-co-vinyl acetate) in Solution

polymer	good solvent conditions	Γ (mg/m ²)	T (°C)	mol wt	solvent	R_g (nm)	C^* (wt %)
PVA-Vac	water at $T < 97$ °C	1.5–2.2	20	10 000	water	3.6	6.3
			20	155 000	water	16	1.1
			80	155 000	water	13	2.1
			20	55 000	water	8	3.1
			80	55 000	water	5.5	9.7

evaporation from the film during the experiments (i.e., to keep a 100% degree of humidity), an excess of solution is located under the porous glass disk during the experiments. The temperature is set to 22 °C and several hours are needed to establish the equilibrium. The experimental setup enables us to measure simultaneously the equilibrium thickness of the film and its disjoining pressure under a constant pressure applied in the box (the disjoining pressure (π) was first introduced by Derjaguin and Obuchov¹⁰ and defined as the excess pressure acting normal to a flat film interface that results from the overlap of molecular interactions between the two adsorbed layers). The film thicknesses are determined by an interferometric method developed by Sheludko.¹¹ The force–distance profiles are calculated from the disjoining pressure–distance profiles by using the Derjaguin approximation.¹

2. Materials Description. The polymer is a statistical copolymer with respectively 88% (or 80% for the lowest molecular weight used in this study: 10 000) of vinyl alcohol (CH₂CHOH) monomers and 12% (20%) of vinyl acetate [CH₂-CH(OCOCH₃)] monomers, which are randomly distributed along the polymer chain. The vinyl alcohol part is hydrophilic, while the vinyl acetate is hydrophobic. This confers some surface properties to this molecule, which adsorbs onto a hydrophobic surface by the randomly distributed monomer on the chain. The adsorption geometry is thus completely different from the case of diblock copolymer-adsorbed at interfaces.¹²

We have worked with three commercial samples (Aldrich Co. and Sigma Co.) with large polydispersity and respective average molecular weight (M_w) 155 000, 55 000 and 10 000. Using a viscosimetric technique, we measure the polymer coils hydrodynamic radii that we assume to be equal to their gyration radius R_g . The values are listed in Table 1 as well as the deduced values of the dilute to semidilute crossover concentrations (C^*). This polymer is water soluble at room temperature (the vinyl alcohol part is hydrophilic and the vinyl acetate is lipophilic). As the temperature increases, water becomes a poorer solvent. The Θ point of PVA-Vac in water is 97 °C.

3. Sample Preparation. The preparation of monodisperse polymer-stabilized emulsions can be performed with PVA-Vac. The process is as follows: an initial polydisperse emulsion, stabilized by sodium dodecyl sulfate (SDS), is first fractionated using several processes described in refs 13 and 7 to obtain a monodisperse emulsion. Then, the emulsion can be strongly concentrated either by centrifugation or by submission to a magnetic field gradient. Then the excedent continuous phase is removed and replaced by the appropriate polymer solution of a given concentration. This procedure can be repeated as many times as needed to completely wash the initial emulsion. In the end, the emulsion bulk phase can be considered as SDS free since, after three “washings”, the SDS concentration does not exceed 10^{−6} M. The obtention of “stable” emulsions is possible in various polymer concentration domains ranging from 0.05% to at least 10% (by weight). The amount of polymer-adsorbed on the emulsion droplets has been determined using a gravimetric measurement technique. The obtained values (from 1.5 to 2.2 mg/m²) are comparable to the adsorbed amount of polymer on solid surfaces (like the mica sheets of the surface force apparatus).^{1,12}

The solutions for both experiments are prepared using only ultrapure water from a Milli Q system. Two kinds of pore size (10–20 and 20–40 μ m) are used for the foam films experiments, depending on flow resistance of the solution and on the disjoining pressure range studied.

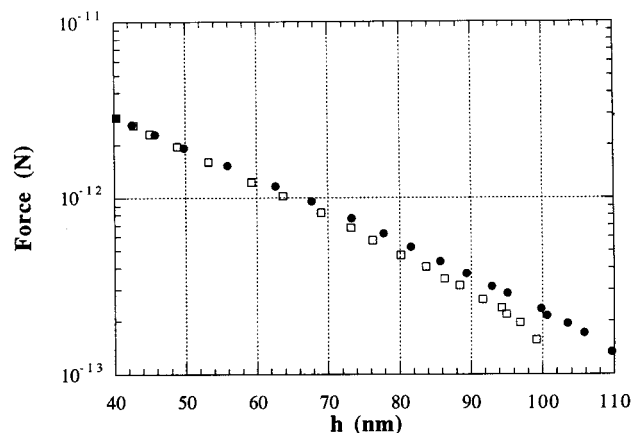


Figure 1. Reversibility of the force–distance profile between emulsion droplets, $M_w = 155$ 000, $C_p = 0.5\%$: (●) force profiles obtained by increasing the applied magnetic field (in); (□) force profiles obtained by decreasing the applied magnetic field (out).

Results and Discussion

1. Compression–Decompression Profiles. We have first checked that the force profiles were fully reversible upon “compression” and “decompression”. By compression and decompression, we mean a measure of the profile with increasing forces and decreasing distances and, opposingly, decreasing forces and increasing distances (see Figure 1 on which no significant hysteresis is observed). The same behavior is observed at the air–water interface. The full reversibility of the profiles contrasts with the results obtained with the surface forces apparatus in similar conditions.^{14,15} This means that the structure of the adsorbed layer is not modified when compressed. In the case of emulsions, a slight hysteresis is observed when approaching the Θ point, i.e., in a zone where the solvent becomes poorer. This is consistent with the appearance of net attractive forces when approaching the bad solvent regime, as seen previously with the SFA technique.⁵

2. Adsorption and Desorption Kinetics. Adsorbed Amounts and Surface Tension. We have evaluated the polymer adsorption and desorption characteristic times by measuring the evolution of the force profiles a few seconds and 3 days after the emulsion preparation. The profile exhibits no significant changes as a function of time, as shown on Figure 2a, meaning that the adsorption time is significantly smaller than the time scale of our experiments (which last typically from 30 min to 1 h).

Whether the polymer adsorbs irreversibly or not at the interface is of considerable importance in the theoretical treatment of polymer forces. To check this point, we have measured the polymer typical desorption time. An emulsion is immersed in a solution of polymer concentration 0.5%. After a sufficient incubation time, the polymer-covered droplets are separated from the continuous phase that is replaced by pure water. The evolution of the force–distance profiles is measured as a function of time (see Figure 2b). Note that this kind

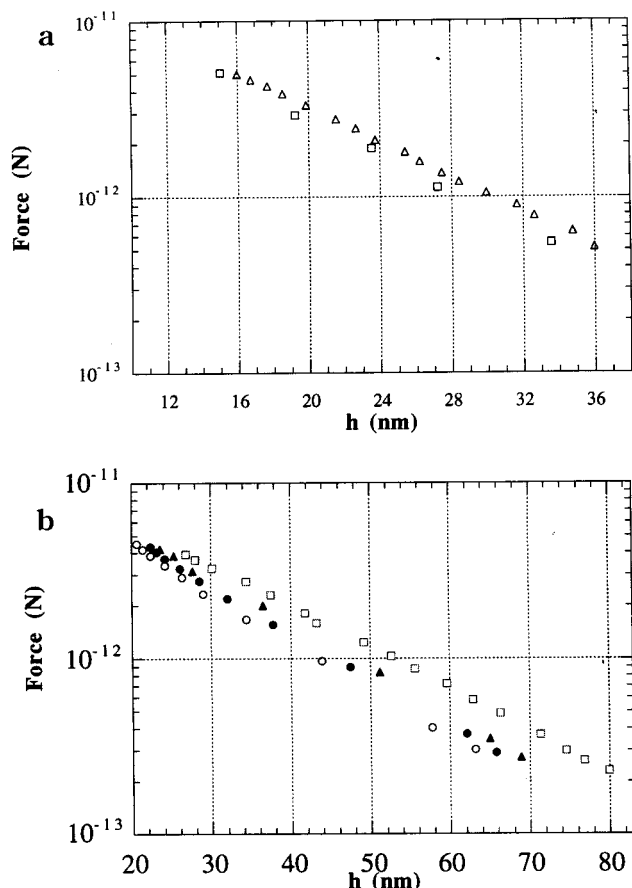


Figure 2. (a) Adsorption kinetics, $M_w = 55\,000$, $C_p = 0.5\%$: (Δ) force profile measured 5 min after the emulsion preparation; (\square) force profile measured 3 days after the emulsion preparation. (b) Desorption kinetics $M_w = 155\,000$: (\square) initial force profile performed in a continuous phase with polymer concentration $C_p = 0.5\%$; force profiles obtained at different times after immersion of the original emulsion droplets in pure water [(Δ) $t = 5$ min; (\bullet) $t = 4$ h; (\circ) $t = 20$ h].

of experiment cannot be performed for foam liquid films, the interfaces being formed during the measurements. The range of the force slightly decreases as a function of time, which can logically be attributed to a desorption of the polymer layer from the interface with a time scale that is typically of tens of hours, i.e., much larger than the time required to perform one experiment (≈ 30 min). Thus, we can consider that, at the time scale of our experiment, the adsorbed amount remains constant and that we explore a regime of irreversible adsorption.

Measurements of the surface tension as function of the bulk polymer concentration lead to the determination of a plateau concentration C_{pl} above which the surface coverage might be considered as constant. The surface tension–bulk concentration curves are plotted in Figure 3a,b for both the oil–water (3a) and the air–water interfaces (3b) and for two molecular weights. We obtain $C_{pl} \approx 0.5\%$ at the oil–water interface and $C_{pl} \approx 4\%$ at the air–water interface. C_{pl} remains roughly constant for the two molecular weights. For $C \geq C_{pl}$, the adsorbed amount at the oil–water interface is equal to $\Gamma \approx 1.5\text{--}2.2$ mg/m², as described in the sample preparation section.

3. Molecular Weight and Concentration Effects.

In Figure 4a,b, we report the influence of the molecular weight on the force–distance profiles at the same polymer bulk concentration (0.5%) with the two tech-

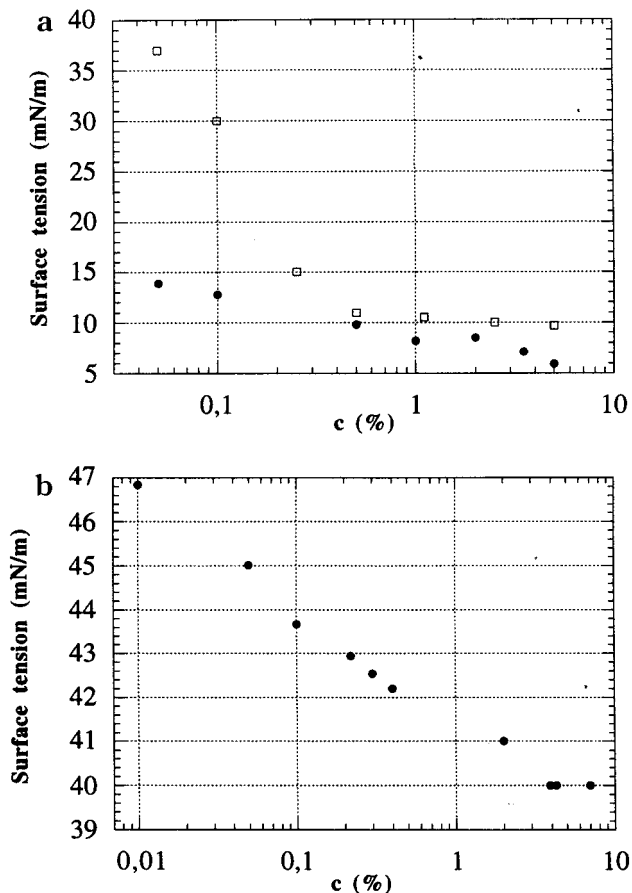


Figure 3. (a) Surface tension measured in PVA–Vac solution at the oil–water interface: (\circ) $M_w = 55\,000$; (\square) $M_w = 155\,000$. Surface tension measured in a PVA–Vac ($M_w = 55\,000$) solution at the air–water interface.

niques. In both cases, we measure repulsive forces in a range of surface separation going roughly from 10 to 100 nm. The profiles systematically reveal an exponential behavior with a decay length that increases with the molecular weight. These results are similar to the one first obtained by Lyklema and van Vliet with the analogue of our foam film measurement technique.⁶ Note also that such behavior was also detected in previous SFA experiments. In previous papers, Luckham and Klein indeed indicate the presence of an exponential regime when the measured forces are very low, i.e., when the polymer-adsorbed layers start to interact one with another.¹⁴ Therefore, our measurements can be considered as an extension of theirs in the regime of low forces and large distances.

The slopes of the semilog plots are roughly identical from one technique to the other. The exponential behavior cannot be attributed to double-layer forces that would be induced by the presence of parasitic charges since the introduction of sodium chloride does not perturb the repulsion (Figure 5). The origin of the force is thus purely steric.

First, we analyze our data with a simple exponential function:

$$F(h) = A \exp(-h/\lambda) \quad (1)$$

where h is the surface separation and λ is the decay length. We have tried to fit our data to a power law with an adjustable exponent, but the agreement is less

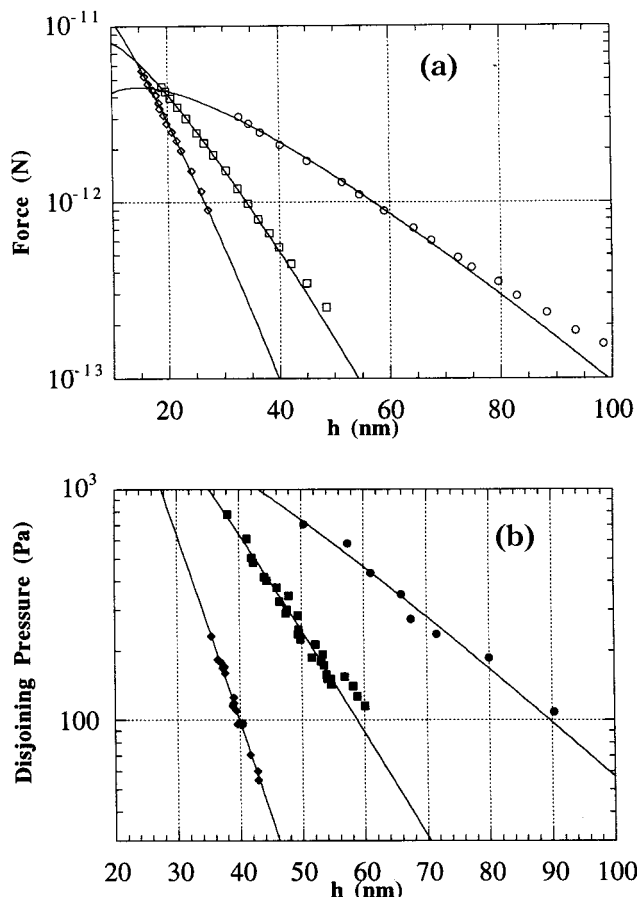


Figure 4. (a) Influence of the polymer molecular weight on the repulsive force–distance profiles between emulsion droplets ($C_p = 0.5\%$): (\diamond) $M_w = 10\,000$; (\square) $M_w = 55\,000$; (\circ) $M_w = 155\,000$. The continuous lines are the best fits to the data using eq 3 in the text. (b) Influence of the polymer molecular weight on the disjoining pressure isotherms at the air–water interface ($C_p = 0.5\%$): (\blacklozenge) $M_w = 10\,000$; (\blacksquare) $M_w = 55\,000$; (\bullet) $M_w = 155\,000$. The continuous lines are the best fits to the data using eq 3 in the text (this equation being adapted for pressure measurements).

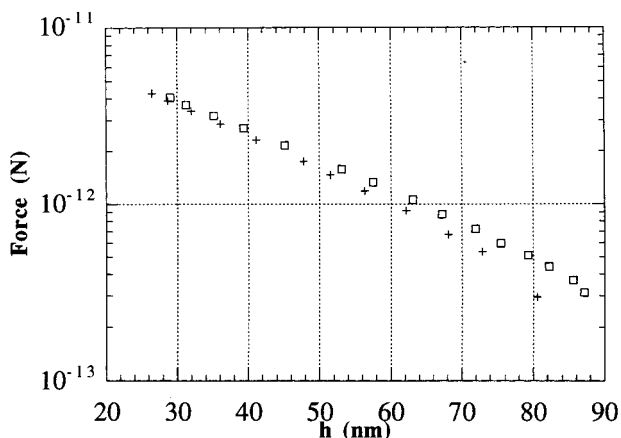


Figure 5. Influence of the continuous phase NaCl concentration on a force–distance profile between emulsion droplets ($M_w = 155\,000$, $C_p = 0.5\%$): (\square) $[\text{NaCl}] = 0\text{ M}$; ($+$) $[\text{NaCl}] = 0.2\text{ M}$.

satisfying than with an exponential. We shall come back to this point further.

A first guess is that the characteristic length λ should scale as the polymer coil gyration radius (R_g). To test this assumption, we have varied the gyration radius by raising the temperature closer to the Θ temperature,

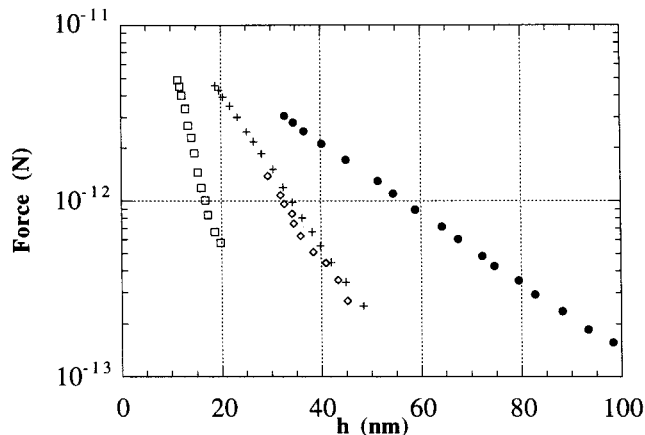


Figure 6. Effect of the temperature on the force–distance profiles between emulsion droplets ($C_p = 0.5\%$): ($+$) $M_w = 55\,000$, $T = 20\text{ }^\circ\text{C}$; (\square) $M_w = 55\,000$, $T = 80\text{ }^\circ\text{C}$; (\bullet) $M_w = 155\,000$, $T = 20\text{ }^\circ\text{C}$; (\diamond) $M_w = 155\,000$, $T = 80\text{ }^\circ\text{C}$.

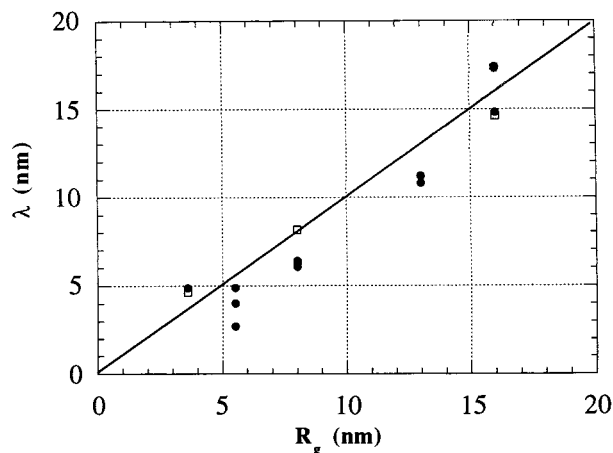


Figure 7. Evolution of the exponential characteristic distance λ (deduced from the best fits to the data using eq 3 in the text) as a function of the polymer coil hydrodynamic radius R_g (deduced from viscosimetric measurements): (\bullet) oil–water interface; (\square) air–water interface.

i.e., in a region where the gyration radius becomes smaller. The evolution of the profiles are plotted in Figure 6. The force range clearly decreases as expected. In Figure 7, we have plotted the evolution of the decay length (λ , fitted to our data with eq 3) as a function of the gyration radius. The two lengths can be considered as linearly related with a slope of around 1.

When fitted to power laws, our data reveal exponents that range from -3 to -4.5 as the investigated force intensities decrease. As previously indicated, our results are similar to the one shown in the pioneering paper of Lyklema and van Vliet.⁶

Looking at the literature, several models predict exponential behaviors. We briefly describe two of these models.

(i) Semenov, Joanny, and Colleagues. Based on the seminal papers of de Gennes,¹⁶ Semenov and co-workers¹⁷ have developed a theory that describes the different force–distance profiles between two polymer-covered walls. The model distinguishes the loop and the tail sections of the adsorbed chains and involves three length scales: the adsorbed layer thickness (λ), an adsorption length z^* that separates the region where the monomer concentration is dominated by loops and by tails, and a microscopic length b inversely propor-

tional to the adsorption strength. In the case of irreversible strong adsorption and good solvent conditions, they predict two kinds of behavior depending on the force–distance regime. Repulsive forces obeying power law functions are expected at short distances, or equivalently large forces, with exponent values that decrease (from -2 to -4) as the separation distance increases. At these distances from the plates, the adsorbed polymer concentration profile is mainly due to loops. Above a given distance (namely λ), the contribution of the polymer tails becomes predominant and the force shifts from a power law to an exponential function with a characteristic decaying length λ that reads

$$\lambda = R_g/(\ln(1/\phi_0 \nu b^2))^{1/2} \quad (2)$$

where ν is the Flory excluded volume parameter and ϕ_0 is the polymer bulk concentration. The force between droplets reads explicitly

$$F(h) = (k_b T \pi R / \lambda^3) h \exp(-h/\lambda) \quad (3)$$

where k_b is the Boltzmann constant, T is the temperature, and R is the droplet radius. Note that this expression is valid only if λ is large enough (essentially larger than z^*), i.e., for a polymer-adsorbed amount close to the saturation value. For smaller adsorbed amounts, the force may become attractive even in cases of irreversible adsorption.

In the weak adsorption limit, the authors claim that the only relevant length scale is the chain radius of gyration, and the adsorbed layer thickness is proportional to it.

(ii) Dolan and Edwards. A similar behavior has been also proposed by Dolan and Edwards.¹⁸ Treating the case of plates covered by end-grafted polymer, the authors predict a positive interaction energy that reads: $E(h) \approx \Gamma \exp(-h/R_g)$ where Γ is the amount of adsorbed polymer. This relation is valid for the large distance ($h > R_g$) and at low surface coverage (low Γ).

We believe that the first model is more adapted to our data since it describes the case of randomly anchored polymers. Thus, as previously described in a recent paper,¹⁹ we have interpreted our data within the frame of the model of Semenov and collaborators, i.e., fitted our data to eqs 2 and 3. We have used the Derjaguin approximation and this model to transform the disjoining pressure into a force. The obtained curves are plotted in Figure 8. As previously indicated, the slopes are very similar from one technique to the other. Also, the force intensities at identical molecular weight are comparable; i.e., the difference never exceeds half a decade. As we argue in section 4, such variation might be due to different adsorbed amounts at the air–water and the oil–water interfaces.

We now compare the theoretical values of the prefactor deduced from eq 3: $k_b T \pi R / \lambda^3$. The results are presented in Table 2 and, considering the precision of our data, the agreement is satisfying. It thus comes out that the measured repulsive force is well described by the model and that, in the large distance regime that we explore, the repulsion is probably due to the polymer tails.

In eq 3, we voluntarily omitted an attractive depletion term that reflects the difference in the solvent chemical potential between the gap separating the interfaces and

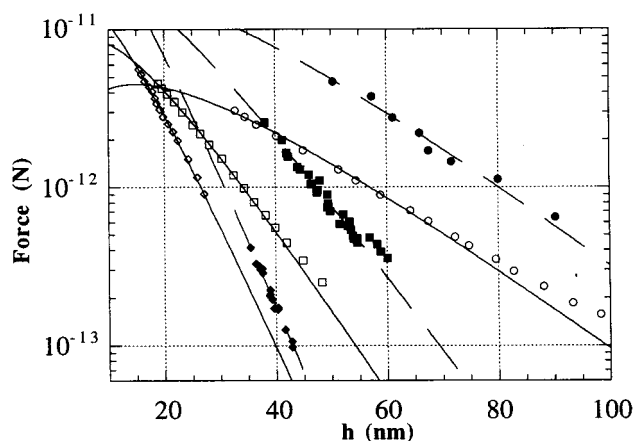


Figure 8. Influence of the polymer molecular weight on the force–distance profiles between oil–water (filled symbols) and air–water interfaces (empty symbols). The pressure–distance data are transformed into forces using the Derjaguin approximation and eq 3 in the text ($C_p = 0.5\%$). Oil–water interface: (\diamond) $M_w = 10\,000$; (\square) $M_w = 55\,000$; (\circ) $M_w = 155\,000$. Air–water interface: (\blacklozenge) $M_w = 10\,000$; (\blacksquare) $M_w = 55\,000$; (\bullet) $M_w = 155\,000$.

Table 2. Compared Values of the Theoretical Prefactor with the Fitted Ones

mol wt	theor prefactor (N/m) $k_b T \pi R / \lambda^3$	fitted prefactor (N/m) (oil–water interface)	fitted prefactor (N/m) (air–water interface)
10 000	10^{-11}	8.4×10^{-12}	2.6×10^{-11}
55 000	3.3×10^{-12}	3.2×10^{-12}	7×10^{-12}
155 000	4×10^{-13}	8.3×10^{-13}	2.9×10^{-12}

the bulk.^{7,20} We can evaluate this term by assuming that the polymer solution behaves as a perfect gas of hard spheres with radius equal to the coil gyration radius (in that case $\pi_{osm} \approx N_a k_b T C_p / M_w$ where N_a is the Avogadro number). Also, we suppose that the polymer free coils are totally expelled from the interface gap as soon as the surface separation becomes lower than their diameter. Following these two assumptions, we obtain a force that is typically of the same order of magnitude as the measured forces and that should be proportional to the bulk polymer concentration. This is clearly not what is observed in Figures 2b and 9a,b where no relevant decreases of the measured forces are observed as the polymer concentration increases. One explanation for this difference with the expected behavior would be that the polymer coils behave as soft spheres and can change their shape to occupy the space between the interfaces. In this respect, the depletion term can be considered as negligible in the concentration range that we explore.

4. Adsorption at the Interfaces. Effect of Added Nonionic Surfactant. In this section, we examine the influence of the polymer-adsorbed amount on the force profiles. As seen in Figure 9b (in the case of foam films), the force intensity slightly increases with the concentration. This effect is not evidenced in the case of ferrofluid emulsion droplets (Figure 9a). We believe that these two different behaviors are due to the different plateau concentration values measured at the two interfaces. From Figure 3a,b, we indeed deduce a plateau concentration C_{pl} above which the surface tension no longer evolves significantly. This means that the polymer surface concentration remains constant above this polymer bulk concentration. As previously mentioned, $C_{pl}(\text{air–water}) > C_{pl}(\text{oil–water})$ and it might be the

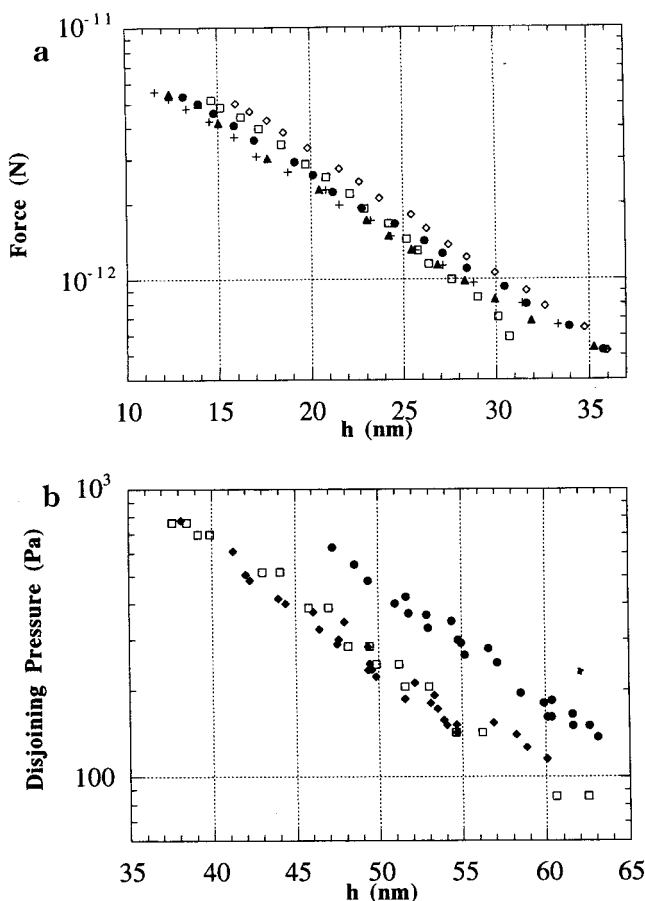


Figure 9. (a) Influence of the polymer concentration on the force–distance profiles between emulsion droplets, $M_w = 55\,000$; (+) $C_p = 0.05\%$; (\blacktriangle) $C_p = 0.08\%$; (\bullet) $C_p = 0.4\%$; (\diamond) $C_p = 1.5\%$; (\square) $C_p = 3.7\%$. (b) Influence of the polymer concentration on disjoining pressure isotherms, $M_w = 55\,000$: (\blacklozenge) $C_p = 0.5\%$; (\square) $C_p = 1\%$; (\bullet) $C_p = 5\%$.

reason why the force intensity slightly increases as the polymer bulk concentration evolves from 0.5% to 5% ($\approx C_{pl}$) in the case of foam films. Oppositely, in the case of emulsion, we do not observe any significant evolution of the force intensities as the bulk concentration is varied from 0.5% to 3.7%, i.e., above the plateau concentration.

To test the variation of the force with the polymer-adsorbed amount (Γ), we have introduced increasing quantities of a nonionic surfactant (nonylphenol oxyethylene NP10 of CMC = 7×10^{-5} M) that is known to adsorb preferentially at the interface and displace the polymer.²¹ The use of nonionic surfactant introduces no long range double-layer forces that would disturb our measurement of steric repulsive forces. In Figure 10a,b, we show the evolution of the disjoining pressure and force–distance profiles with increasing NP10 concentrations. The characteristic distance λ remains unchanged, while the preexponential factor decreases with the polymer-adsorbed amount. The same behavior is observed in both cases. Above a given NP10 concentration, the exponential profile vanishes and the equivalent of a “hard sphere” behavior is measured. However, the concentration above which the profile becomes “hard sphere” (C_{hs}) varies from one interface to the other (from $C_{hs} = \text{CMC}$ at the oil–water interface to $C_{hs} = 3 \text{ CMC}$ at the air–water interface). The different values of C_{hs} reveal a difference in the polymer-adsorbed amount and adsorbing strength from one interface to the other, thus

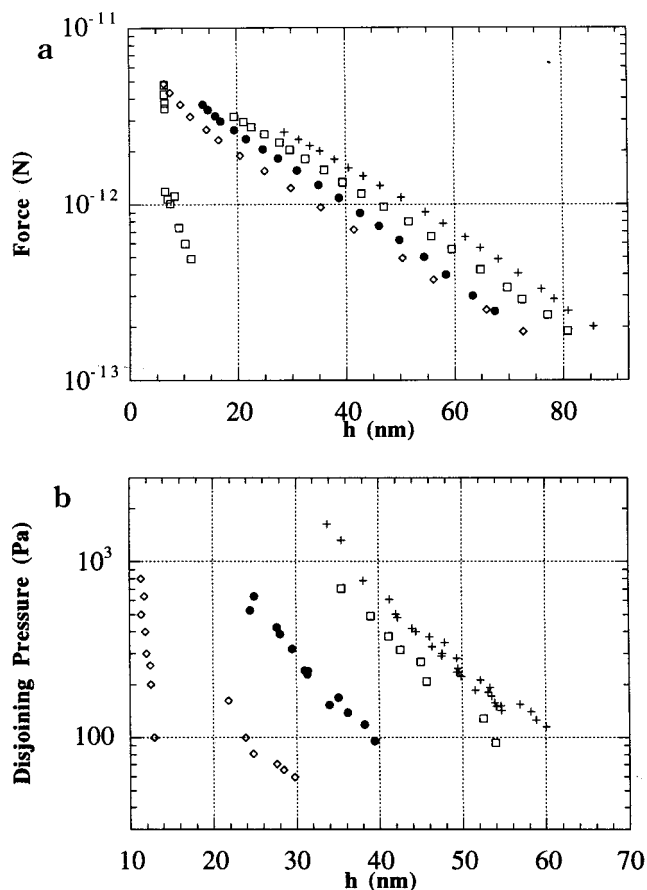


Figure 10. (a) Influence of a nonionic surfactant concentration (NP10 of CMC = 7×10^{-5} M) on the force–distance profiles between emulsion droplets ($C_p = 0.5\%$; $M_w = 155\,000$): (+) [NP10] = 0 M; (\square) [NP10] = CMC/20; (\bullet) [NP10] = CMC/10; (\diamond) [NP10] = CMC/3; (\square) [NP10] = CMC. (b) Influence of NP10 concentration (CMC = 7×10^{-5} M) on the pressure isotherms ($C_p = 0.5\%$; $M_w = 55\,000$): (+) [NP10] = 0 M; (\square) [NP10] = CMC/10; (\bullet) [NP10] = CMC; (\diamond) [NP10] = 3 CMC.

confirming our hypothesis that the force intensities are connected to Γ . Also, a discontinuous profile, typical of structuration effects, is detected in the foam film at $C = 3 \text{ CMC}$, due to the trapping of micelles between the interfaces.²² This structuration was never observed in the case of emulsions, even at higher surfactant concentration,⁷ probably because of curvature effects (the droplet/micelle radius ratio is typically around 10, while it is quasi infinite in the case of foam films).

Such evolution of forces as function of Γ is incompatible with the prediction of Semenov and co-workers in the large adsorption regime in which the force prefactor is supposed to vary very smoothly with Γ . This suggests that, in the presence of surfactant, the experimental conditions are those of an intermediate adsorption regime. This regime tends to be similar to the one described by Dolan and Edwards in which the force prefactor is directly proportional to Γ .

Conclusion

We have probed the forces that arise between polymer-covered fluid interfaces in good solvent conditions. In the absence of any added surfactant, the neutral statistical copolymer is shown to adsorb irreversibly at the interface but gives rise to fully reversible force–distance profiles upon compression and decompression. By varying the polymer molecular weight and solvent condi-

tions, our measurements reveal exponential profiles with characteristic distances that scale as the free coil gyration radius. This length is insensitive to the polymer bulk concentration and to the nature of the fluid–fluid interface since no significant qualitative differences are observed between air–water and oil–water interfaces. When compared to previous experimental results obtained between solid surfaces, our data fit well with the lowest force intensity regime that was probed with the surface forces apparatus. Therefore, we believe that the main differences between the SFA results and ours are due to the different regimes of forces intensities that are probed with these techniques.

The force intensity is slightly different between the two techniques used in this study. By varying the polymer-adsorbed amount Γ through the use of a surfactant that displaces it from the interface, we demonstrate that the force intensity is a direct (though unknown) function of Γ and thus depends on the nature of the interface.

Comparing our results to the different theories on polymer-induced forces, it seems that our data fit quite well with the predictions of Semenov and collaborators. The authors indeed expect such an exponential behavior with a length proportional to R_g , as we observe. Also, evaluations of the forces prefactors lead to values comparable to the ones deduced from the fit to our data. A disagreement appears when the polymer-adsorbed amount is decreased, which is not surprising since their predictions refer to a large adsorption regime. Therefore, we believe that the observed discrepancies are mainly due to the fact that we probe a regime of intermediate adsorption strength that does not fully enter the theoretically treated strong adsorption limiting case. Oppositely, in this weak adsorption limit, our results compare well with the predictions of Dolan and Edwards in which the force prefactor is directly proportional to the adsorbed amount Γ .

Acknowledgment. We thank J.-F. Joanny, J. Philip, A. Colin and D. Roux for fruitful and stimulating discussions.

References and Notes

- (1) Israelachvili, J. *Intermolecular and Surface Forces*; Academic: San Diego, 1985.
- (2) Napper, D. H. *Polymeric Stabilization of Colloidal Dispersions*; Academic Press: London, 1989.
- (3) Leal Calderon, F.; Stora, T.; Mondain-Monval, O.; Poulin, P.; Bibette, J. *Phys. Rev. Lett.* **1994**, *72*, 865.
- (4) Claesson, P. M.; Ederth, T.; Bergeron, V.; Rutland, M. W. *Adv. Colloid Interface Sci.* **1996**, *68*, 119.
- (5) Patel, S. S.; Tirrell, M. *Annu. Rev. Phys. Chem.* **1989**, *40*, 597.
- (6) Lyklema, J.; Van Vliet, T. *Faraday Discuss. Chem. Soc.* **1978**, *65*, 26.
- (7) Mondain-Monval, O.; Leal Calderon, F.; Bibette, J. *J. Phys. II (France)* **1996**, *6*, 1313.
- (8) Mysels, K. M.; Jones, N. *Discuss. Faraday Soc.* **1966**, *42*, 50.
- (9) Bergeron, V.; Radke, C. J. *Langmuir* **1992**, *8*, 3020. Espert, A.; von Klitzing, R.; Poulin, P.; Colin, A.; Zana, R.; Langevin, D. *Langmuir*, **1998**, *14*, 4251.
- (10) Derjaguin, B. V.; Obuchov, E. *Acta Physiochim. URSS* **1936**, *5*, 1.
- (11) Sheludko, A. *Adv. Colloid Interface Sci.* **1967**, *1*, 391.
- (12) Fleer, G.; Cohen Stuart, M.; Scheutjens, J.; Cosgrove, T.; Vincent, B. *Polymers at Interfaces*; Chapman and Hall: London, 1993.
- (13) Bibette, J. *J. Colloid Interface Sci.* **1991**, *147*, 474.
- (14) Luckham, P. F.; Klein, J. *Nature* **1982**, *300*, 429. *Macromolecules* **1984**, *17*, 1041; **1985**, *18*, 721; *J. Chem. Soc., Faraday Trans.* **1990**, *86*, 1363.
- (15) Lubetkin, S. *Colloid Surf.* **1988**, *31*, 203.
- (16) de Gennes, P. G. *Macromolecules* **1981**, *14*, 1637; **1982**, *15*, 492; *Scaling Concepts in Polymer Physics*; Cornell University Press: London, 1979.
- (17) Semenov, A. N.; Bonet-Avalos, J.; Johnner, A.; Joanny, J.-F. *Macromolecules* **1996**, *29*, 2179; **1997**, *30*, 1479.
- (18) Dolan, A. K.; Edwards, S. F. *Proc. R. Soc. London* **1974**, *337*, 509.
- (19) Mondain-Monval, O.; Espert, A.; Omarjee, P.; Bibette, J.; Leal-Calderon, F.; Philip, J.; Joanny, J.-F. *Phys. Rev. Lett.* **1998**, *80*, 1778.
- (20) de Hek, H.; Vrij, A. *J. Colloid Interface Sci.* **1982**, *88*, 258. Richetti, P.; Kékicheff, P. *Phys. Rev. Lett.* **1992**, *68*, 1951. Mondain-Monval, O.; Leal-Calderon, F.; Philip, J.; Bibette, J. *Phys. Rev. Lett.* **1995**, *75*, 3364.
- (21) Sonntag, H.; Unterberger, B.; Zimontkowski, S. *Colloid Polym. Sci.* **1979**, *257*, 286.
- (22) Exerowa, D.; Kolarov, T.; Kristov, K. H. R. *Colloid Surf.* **1987**, *22*, 171.

MA980330S